Journal of Inorganic and General Chemistry
ZAAC
Zeitschrift für anorganische und allgemeine Chemie
www.zaac.wiley-vch.de
ARTICLE

DOI: 10.1002/zaac.201500271

Syntheses, Crystal Structures, and Thermal Expansion Properties of Three-Dimensional Cyanide-Bridged Compounds $Zn(4,4'\text{-bpy})(H_2O)_2M(CN)_4$ (4,4′-bpy = 4,4′-bipyridine; *M* = Ni, Pd, Pt)

Xiao-Yan Tian,[a] Ai-Yun Hu,[a] Ai-Hua Yuan,*[a] Qi Chen,[a] Dan Yang,[a] and Fei-Lin Yang[a]

Keywords: Cyanide-bridging; Zinc; Nickel; Palladium; Platinum; Thermal expansion

Abstract. Three cyanide-bridged compounds $Zn(4,4'\text{-bpy})(H_2O)_2M(CN)_4$ (4,4′-bpy = 4,4′-bipyridine; *M* = Ni (**1**), Pd (**2**), Pt (**3**)) were synthesized by self-assembly of Zn^{2+} ions, pillar ligands 4,4′-bpy and $[M(CN)_4]^{2-}$. Single-crystal X-ray diffraction analysis revealed that compounds **1**–**3** are isostructural and belong to monoclinic space group *C*2/*c*. The zinc atom is located in a distorted octahedral arrangement, whereas the central nickel atom adopts square-planar arrangement. The central Zn and Ni atoms are linked alternatingly through two *cis* cyanide groups, generating zigzag chains. The adjacent chains are further connected along two different directions by 4,4′-bpy ligands to form a three-dimensional framework. Thermal expansion (TE) analyses of compounds **1**–**3** showed that both *a* and *c* axes are positive TE coefficients, compared to the near zero TE one along the *b* axis.

Introduction

Coordination compounds have attracted much attention because of their tremendous potential applications.[1] Cyanometalates are widely employed to act as flexible building blocks to construct various types of polymeric networks, and these materials have exhibited intriguing properties such as magnetism, host-guest interactions, gas storage, and so on.[2–5] Recently, thermal expansion (TE) properties of cyanide-based system have received particular attention. Typical examples include the discovery of the most pronounced isotropic negative TE reported in single network $Cd(CN)_2$,[6] the greatest anisotropic negative TE observed in $Ag_3[Co(CN)_6]$,[7] the tuning of TE by metal site substitution,[8,9] and guest inclusion.[10–12] The negative TE behavior in these frameworks originates from a transverse vibrational mechanism analogous to that of the oxides. Notably, a zero TE material $Rb_{0.7}Mn[Fe(CN)_6]_{0.99}\cdot 0.3H_2O$ was reported by the *Ohkoshi* group.[13] In fact, tetracyanide-bearing precursors $[M(CN)_4]^{2-}$ (*M* = Ni, Pd, Pt) have been widely used to construct multi-functional coordination compounds and the resulting materials exhibited interesting properties such as spin-crossover, photomagnetism, porosity, etc.[14–18] However, studies on the TE properties of tetracyanometalate-based coordination compounds have been reported limitedly.

In order to further investigate TE properties for $[M(CN)_4]^{2-}$-based systems, the three-dimensional compounds $Zn(4,4'\text{-bpy})(H_2O)_2M(CN)_4$ (4,4′-bpy = 4,4′-bipyridine; *M* = Ni (**1**), Pd (**2**), Pt (**3**)) were isolated by self-assemblies of transition metal ions Zn^{2+}, pillar ligands 4,4'-bpy and $[M(CN)_4]^{2-}$ and their syntheses, structures, and TE properties are reported herein.

Results and Discussion

Single-crystal X-ray diffraction analysis revealed that compounds **1**–**3** are isostructural and crystallize in the monoclinic space group *C*2/*c* (Table 1, Figure 1, Figure S4, Figure S5, Supporting Information). Therefore, only the structure of compound **3** is described in detail.

The asymmetric unit of compound **3** contains one $[Zn(4,4'\text{-bpy})(H_2O)_2]^{2+}$ cation and one $[Pt(CN)_4]^{2-}$ anion. The Zn atom is located on an inversion center, whereas Pt sits on a twofold rotation axis. The central zinc atom adopts a distorted octahedral $\{ZnN_4O_2\}$ arrangement, where the six positions are occupied by four nitrogen atoms from two cyanide groups and two 4,4′-bpy ligands. The axial positions are occupied by two coordinated water molecules. The average Zn–O and Zn–N lengths are 2.184(7) Å and 2.132 Å, respectively (Table 2). The $[Pt(CN)_4]^{2-}$ anion exhibits a square-planar arrangement, in which two *cis* cyanide groups acting as linkers bridged to adjacent Zn sites and the others are terminal.

As a result, the central Zn and Ni atoms are linked alternatively through two *cis* cyanide groups to generate zigzag chains (Figure 2a). The intrachain Zn···*M*, Zn···Zn, and *M*···*M* distances are 5.247 Å, 7.390 Å, and 10.494 Å for compound **3**, respectively (5.129, 7.227, and 10.258 Å for compound **1**;

* Prof. Dr. A.-H. Yuan
E-Mail: aihuayuan@163.com
[a] School of Environmental and Chemical Engineering
Jiangsu University of Science and Technology
Zhenjiang 212003, P. R. China
Supporting information for this article is available on the WWW under **http://dx.doi.org/10.1002/zaac.201500271** or from the author.

Table 1. Crystallographic data and structural refinement for compounds **1**–**3**.

	1	**2**	**3**
Formula	$ZnNiC_{14}H_{12}N_6O_2$	$ZnPdC_{14}H_{12}N_6O_2$	$ZnPtC_{14}H_{12}N_6O_2$
M_r	420.38	468.07	556.76
Crystal system	monoclinic	monoclinic	monoclinic
Space group	*C*2/*c*	*C*2/*c*	*C*2/*c*
a /Å	15.329(5)	15.6500(19)	15.695(5)
b /Å	14.930(5)	15.1604(18)	15.172(5)
c /Å	7.426(2)	7.3062(9)	7.262(2)
β /°	110.899(4)	110.650(10)	110.712(4)
V /Å^3	1587.8(9)	1621.9(3)	1617.6(9)
Z	4	4	4
ρ /g·cm^{-3}	1.759	1.917	2.286
Total, unique	5898, 1493	6081, 1529	7070, 1898
F(000)	848	920	1048
Observed [$I > 2\sigma(I)$]	1312	1434	1379
GOF on F^2	1.050	1.055	0.924
R_1, wR_2 [$I > 2\sigma(I)$]	0.0224, 0.0539	0.0197, 0.0478	0.0535, 0.1205
R_1, wR_2 (all data)	0.0274, 0.0552	0.0217, 0.0486	0.0571, 0.1214

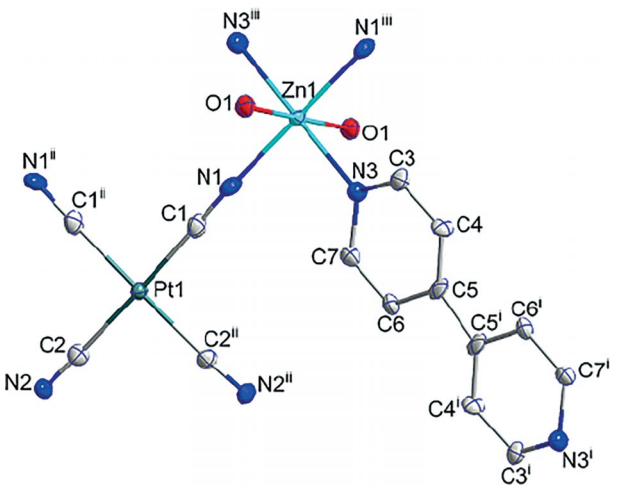

Figure 1. Molecular structure of compound **3** with displacement ellipsoids drawn at the 30 % probability level (all hydrogen atoms were omitted for clarity). Symmetry codes: (i) –*x*, –*y*, –*z*+1; (ii) –*x*+1, *y*, –*z*+5/2; (iii) –*x*+1/2, –*y*+1/2, –*z*+2.

Table 2. Selected bond lengths /Å and angles /° for compounds **1**–**3**.

	1	**2**	**3**
Zn1–N1	2.1183(18)	2.102(2)	2.108(9)
Zn1–N3	2.1366(16)	2.1777(18)	2.155(8)
Zn1–O1	2.2236(15)	2.1935(16)	2.184(7)
*M*1–C1	1.865(2)	1.992(2)	1.966(11)
*M*1–C2	1.876(2)	2.001(2)	2.022(10)
N1–C1	1.156(3)	1.155(3)	1.178(14)
N2–C2	1.148(3)	1.152(3)	1.089(13)
*M*1–C1–N1	178.50(19)	178.1(2)	179.3(10)
*M*1–C2–N2	178.2(2)	178.6(2)	174.7(10)
Zn1–N1–C1	172.59(19)	173.4(2)	174.8(9)

5.241, 7.376, and 10.481 Å for compound **2**). These chains are further connected by 4,4′-bpy ligands along two different directions, forming a three-dimensional (3D) framework (Figure 2b). The cavities are filled by coordinated water molecules. The structural feature of compounds **1**–**3** are obviously different to those observed in 3D Hofmann-type system, where cyanide-based layers are linked by pillar ligands to generate a 3D open network and the resulting materials have exhibited excellent properties.[19–22]

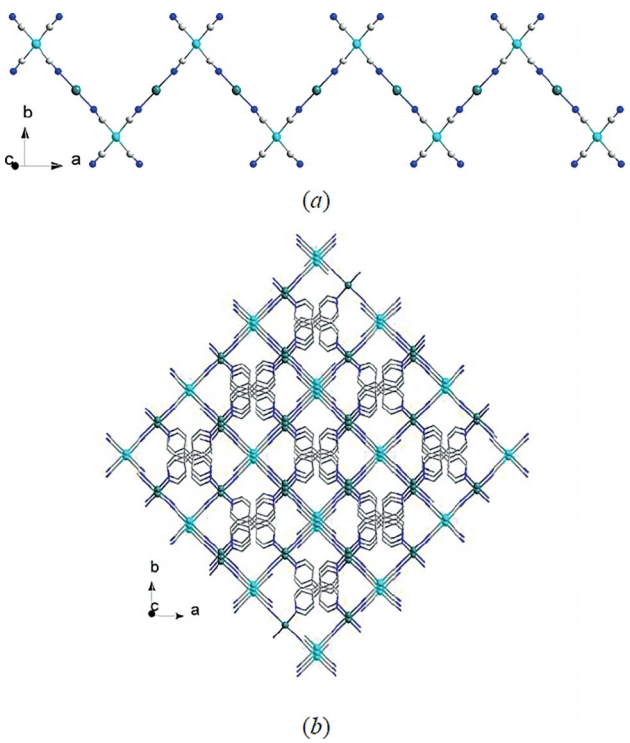

Figure 2. (a) Zigzag chain of compound **3** (all hydrogen atoms, oxygen atoms and 4,4′-bpy ligands are omitted for clarity). (b) 3D framework of compound **3** (all hydrogen and oxygen atoms are omitted for clarity).

Powder X-ray diffraction analysis (Figure S6, Supporting Information) of compound **3** indicated the high purity of as-synthesized polycrystalline samples. TG curve (Figure S7) showed no further mass up to about 125 °C due to the absence of crystallized guest molecules in the structure. A well-pronounced weight loss stage was detected when temperatures were increased, which corresponds to the coordinated water

molecule. The framework began to collapse upon further increasing temperatures.

The thermal expansion (TE) behaviors of compounds **1–3** were measured using variable temperature single-crystal X-ray diffraction to monitor the lattice parameters as a function of temperature (Figure 3, Figure S8 and Figure S9). Variable temperature single crystal unit cell determinations were performed by continuously collecting matrix files as the collection temperature was varied at a rate of 10 K·h^{-1} from 100 K to 350 K. The TE coefficients of unit cell parameters *a*, *b*, *c* and *V* are shown in Table 3. Only the TE properties of compound **3** are described herein because compounds **1–3** exhibited similar TE features. The TE coefficients parallel to the *a* and *c* axes for compound **3** are positive with values of 67.7×10^{-6} K^{-1} and 92.2×10^{-6} K^{-1}, respectively. Interestingly, the very low value (-0.3×10^{-6} K^{-1}) were observed parallel to the *b* axis over a wide temperature range of 100–350 K, and thus the TE coefficient along the *b* axis can be considered as zero. The TE coefficients parallel to the *b* axis for compounds **1–3** are considerably smaller than the large negative TE effect [α_a = -33.5×10^{-6} K^{-1} for $Cd(CN)_2$ and $\alpha_a = (-120$ to $-130) \times 10^{-6}$ K^{-1} for $Ag(CN)_6$].[6,7] It should be noted that compound **3** exhibited positive TE behavior because of the obviously positive value (118×10^{-6} K^{-1}) for volume TE coefficient. The pronounced anisotropic TE behaviors parallel to three unit cell axis for compounds **1–3** are rare in cyanide-based materials with unique TE behaviors. By comparison, some cyanide-based materials have also shown interesting properties of zero TE with coefficients in all unit cell parameters (*a*, *b*, *c*, and *V*) of α_a = $+0.2 \times 10^{-6}$ K^{-1} (300–20 K) for $Cs^{I}_{0.94}Mn^{II}[Fe^{II}(CN)_6]_{0.21}[Fe^{III}(CN)_6]_{0.70}\cdot 0.80H_2O$, $+0.67 \times 10^{-6}$ K^{-1} (368–218 K) for $N(CH_3)_4CuZn(CN)_4$, and -1.47×10^{-6} K^{-1} (300–4.2 K) for $Fe[Co(CN)_6]$.[23–25] Generally, the negative TE behaviors observed in cyanide-based materials can be ascribed to the low-energy transverse vibration modes of δ(*M*–C≡N–*M*′), which reduced the average metal-metal distances, and thus the lattice parameters with increasing temperature.[7,26,27] However, the zero TE effect parallel to the *b* axis for compounds **1–3** may be attributed to the fact that coordinated water molecules in the interstitial sites lead to steric dampening of the transverse modes of δ(*M*–C≡N–Zn), which limits the contraction coefficients. In addition, the obviously different TE properties parallel to the *a* and *b* axis were probably caused by the different coordinatively bonding directions along two axis.

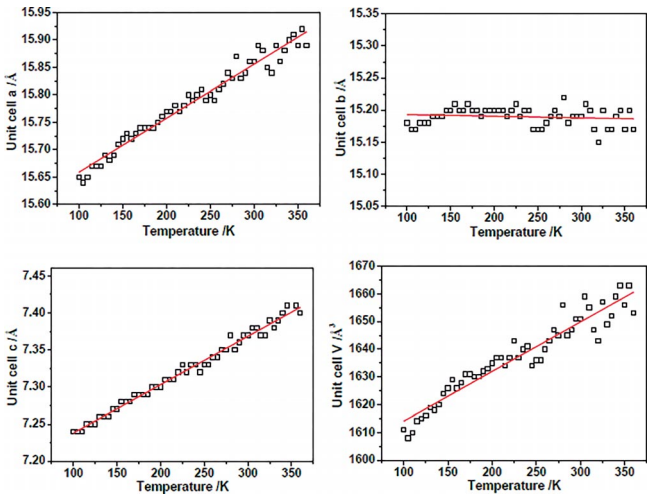

Figure 3. Temperature dependence of the lattice constants, *a*, *b*, *c*, and *V* for compound **3**.

Table 3. Thermal expansion coefficients of compounds **1–3**.

	α_a /$\times 10^{-6}$ K^{-1}	α_b /$\times 10^{-6}$ K^{-1}	α_c /$\times 10^{-6}$ K^{-1}	α_v /$\times 10^{-6}$ K^{-1}
1	60.8	4.5	92.7	123.3
2	63.3	–1.6	90.1	112
3	67.7	–0.3	92.2	118

Conclusions

Three isostructural 3D tetracyanometalate-based compounds were isolated and characterized. The presence of pillar ligands during the synthesis process is practically responsible for the formation of high-dimensional architectures. Interestingly, obviously different and unique TE behaviors were observed parallel to three unit cell axis, which enriched the content of cyanide-based materials with unique properties. Further work on the mechanism responsible for the anomalous TE behaviors in these compounds is underway.

Experimental Section

Materials and General Methods: All reagents, unless otherwise stated, were obtained from commercial sources and were used without further purification. Elemental analyses for C, H, and N were performed with a Perkin-Elmer 240C elemental analyzer. IR spectra were measured with a Nicolet FT 1703X spectrophotometer in the form of KBr pellets in the 4000–400 cm^{-1} region. Powder X-ray diffraction patterns were collected at 4°·min^{-1} with Cu-K_α radiation using a Shimadzu XRD-6000 diffractometer. Thermogravimetry (TG) analyses were carried out at a ramp rate of 15 K·min^{-1} in a nitrogen atmosphere with a Perkin-Elmer Pyris Diamond TGA analyzer.

Syntheses of $Zn(4,4'\text{-bpy})(H_2O)_2M(CN)_4$ [*M* = Ni (1), Pd (2), Pt (3)]: Single crystals of compounds **1–3** were prepared at room temperature by slow diffusion of an EtOH/H_2O solution (v/v = 1/1) (2 mL) containing $ZnSO_4\cdot 7H_2O$ (0.05 mmol) and 4,4′-bpy (0.05 mmol) into an EtOH/H_2O solution (v/v = 1/1) (20 mL) of $K_2[M(CN)_4]$ [*M* = Ni (**1**), Pd (**2**), Pt (**3**)] (0.05 mmol). Pale yellow (**1**) or colorless (**2**, **3**) rod-shaped crystals were obtained after about 20 d. Yield for compound **1**: 39% based on the Zn salt. Compounds **2** and **3** have similar mass yields to compound **1**. $ZnNiC_{14}H_{12}N_6O_2$ (**1**): calcd. C 40.00; H 2.88; N 19.99%; found: C 38.99; H 2.92; N 20.12%. $ZnPdC_{14}H_{12}N_6O_2$ (**2**): calcd. C 35.92; H 2.58; N 17.95%; found: C 36.15; H 2.51; N 17.77%. $ZnPtC_{14}H_{12}N_6O_2$ (**3**): calcd. C 30.20; H 2.17; N 15.09%; found: C 30.33; H 2.12; N 15.01%. **IR** (KBr): $\tilde{\nu}$ = (for compound **1**) ν(C≡N) 2193, 2160, 2129, 2116 cm^{-1}; (for compound **2**) ν(C≡N) 2189, 2177, 2145, 2131 cm^{-1}; (for compound **3**) ν(C≡N) 2191, 2175, 2143, 2098 cm^{-1} (Figures S1–S3, Supporting Information)

X-ray Crystallographic Analysis: Diffraction data for compounds **1–3** were collected with a Bruker Smart APEX II diffractometer equipped with Mo-K_α (λ = 0.71073 Å) radiation. Diffraction data analysis and

reduction were performed within SMART, SAINT, and XPREP.[28] Correction for Lorentz, polarization, and absorption effects were performed within SADABS.[29] Structures were solved using Patterson method within SHELXS-97 and refined using SHELXL-97.[30–32] All non-hydrogen atoms were refined with anisotropic thermal parameters. The hydrogen atoms of 4,4′-bpy were calculated at idealized positions and included in the refinement in a riding mode. The hydrogen atoms bound to coordinated water molecule were located from difference Fourier maps and refined as riding mode.

Crystallographic data (excluding structure factors) for the structures in this paper have been deposited with the Cambridge Crystallographic Data Centre, CCDC, 12 Union Road, Cambridge CB21EZ, UK. Copies of the data can be obtained free of charge on quoting the depository numbers CCDC-1055555 (**1**), CCDC-1055556 (**2**), and CCDC-1055557 (**3**) (Fax: +44-1223-336-033; E-Mail: deposit@ccdc.cam.ac.uk, http://www.ccdc.cam.ac.uk).

Supporting Information (see footnote on the first page of this article): IR spectra of compounds **1**–**3**. ORTEP diagrams and the temperature dependence of the lattice constants of compounds **1** and **2**; Powder XRD pattern and TG curve of compound **3**, Temperature dependence of the lattice constants, *a*, *b*, *c*, and *V* for compounds **1** and **2**.

Acknowledgements

The authors are grateful for financial support from the National Natural Science Foundation of China (51072072, 51272095), and Qing Lan Project of Jiangsu Province.

References

[1] J.-P. Zhang, X.-M. Chen, *Struct. Bonding (Berlin)* **2014**, *157*, 1–26.
[2] B. Nowicka, T. Korzeniak, O. Stefańczyk, D. Pinkowicz, S. Chorąży, R. Podgajny, B. Sieklucka, *Coord. Chem. Rev.* **2012**, *256*, 1946–1971.
[3] H. Tokoro, S. Ohkoshi, *Dalton Trans.* **2011**, *40*, 6825–6833.
[4] M. Shatruk, C. Avendano, K. R. Dunbar, *Prog. Inorg. Chem.* **2009**, *56*, 155–334.
[5] A. H. Yuan, H. Zhou, G. W. Diao, P. D. Southon, C. J. Kepert, L. Liu, *Int. J. Hydrogen Energ.* **2014**, *39*, 884–889
[6] A. E. Phillips, A. L. Goodwin, G. J. Halder, P. D. Southon, C. J. Kepert, *Angew. Chem. Int. Ed.* **2008**, *47*, 1396–1399.
[7] A. L. Goodwin, M. Callaja, M. J. Conterio, M. T. Dove, J. S. O. Evans, D. A. Keen, L. Peters, M. G. Tucker, *Science* **2008**, *319*, 794–797.
[8] K. W. Chapman, P. J. Chupas, C. J. Kepert, *J. Am. Chem. Soc.* **2006**, *128*, 7009–7014.
[9] S. G. Duyker, V. K. Peterson, G. J. Kearley, A. J. Ramirez-Cuesta, C. J. Kepert, *Angew. Chem. Int. Ed.* **2013**, *52*, 5266–5270.
[10] A. L. Goodwin, K. W. Chapman, C. J. Kepert, *J. Am. Chem. Soc.* **2005**, *127*, 17980–17981.
[11] A. L. Goodwin, B. J. Kennedy, C. J. Kepert, *J. Am. Chem. Soc.* **2009**, *131*, 6334–6335.
[12] T. Pretsch, K. W. Chapman, G. J. Halder, C. J. Kepert, *Chem. Commun.* **2006**, 1857–1859.
[13] H. Tokoro, K. Nakagawa, K. Imoto, F. Hakoe, S. I. Ohkoshi, *Chem. Mater.* **2012**, *24*, 1324–1330.
[14] S. L. Zhang, X. H. Zhao, Y. M. Wang, D. Shao, X. Y. Wang, *Dalton Trans.* **2015**, *44*, 9682–9690.
[15] L. Piñeiro-López, M. Seredyuk, M. C. Muñoz, J. A. Real, *Chem. Commun.* **2014**, *50*, 1833–1835.
[16] N. F. Sciortino, S. M. Neville, J. F. Letard, B. Moubaraki, K. S. Murray, C. J. Kepert, *Inorg. Chem.* **2014**, *53*, 7886–7893.
[17] J. T. Culp, C. Madden, K. Kauffman, F. Shi, C. Matranga, *Inorg. Chem.* **2013**, *52*, 4205–4216.
[18] N. F. Sciortino, K. R. Scherl-Gruenwald, G. Chastanet, G. J. Halder, K. W. Chapman, J. F. Létard, C. J. Kepert, *Angew. Chem. Int. Ed.* **2012**, *51*, 10154–10158.
[19] N. F. Sciortino, S. M. Neville, J. F. Létard, B. Moubaraki, K. S. Murray, C. J. Kepert, *Inorg. Chem.* **2014**, *53*, 7886–7893.
[20] L. Piñeiro-López, M. Seredyuk, M. C. Muñoz, J. A. Real, *Chem. Commun.* **2014**, *50*, 1833–1835.
[21] M. M. Deshmukh, M. Ohba, S. Kitagawa, S. Sakaki, *J. Am. Chem. Soc.* **2013**, *135*, 4840–4849.
[22] C. Bartual-Murgui, A. Akou, H. J. Shepherd, G. Molnár, J. A. Real, L. Salmon, A. Bousseksou, *Chem. Eur. J.* **2013**, *19*, 15036–15043.
[23] A. E. Phillips, G. J. Halder, K. W. Chapman, A. L. Goodwin, C. J. Kepert, *J. Am. Chem. Soc.* **2010**, *132*, 10–11.
[24] T. Matsuda, H. Tokoro, K. Hashimoto, S. Ohkoshi, *Dalton Trans.* **2006**, 5046–5050.
[25] S. Margadonna, K. Prassides, A. N. Fitch, *J. Am. Chem. Soc.* **2004**, *126*, 15390–15391.
[26] A. L. Goodwin, C. J. Kepert, *Phys. Rev. B* **2005**, *71*, 140301.
[27] K. W. Chapman, P. J. Chupas, C. J. Kepert, *J. Am. Chem. Soc.* **2005**, *127*, 15630–15636.
[28] Bruker, *SMART*, *SAINT* and *XPREP*, Area Detector Control and Data Integration and Reduction Software, Bruker Analytical X-ray Instruments Inc., Madison, WI, USA, **1995**.
[29] G. M. Sheldrick, *SADABS*, Empirical Absorption and Correction Software, University of Göttingen, Göttingen, Germany, **1996**.
[30] G. M. Sheldrick, *SHELXS-97*, Program for X-ray Crystal Structure Solution, University of Göttingen, Göttingen, Germany, **1997**.
[31] G. M. Sheldrick, *SHELXL-97*, Program for X-ray Crystal Structure Refinement, University of Göttingen, Göttingen, Germany, **1997**.
[32] G. M. Sheldrick, *Acta Crystallogr., Sect. A* **2008**, *64*, 112–122.

Received: May 24, 2015
Published Online: August 19, 2015

